JACS
JOURNAL OF THE AMERICAN CHEMICAL SOCIETY
pubs.acs.org/JACS

Open Access
This article is licensed under CC-BY-NC-ND 4.0

Article

Sterically Induced Acceleration of Aryl Halide Activation by Pd(0): A Radical Alternative to 2-Electron Oxidative Addition

Daniel Hupperich, Jaime Ponce-de-León, Ignacio Funes-Ardoiz, Theresa Sperger, and Franziska Schoenebeck*

Cite This: J. Am. Chem. Soc. 2025, 147, 19941−19948

Read Online

ACCESS | Metrics & More | Article Recommendations | Supporting Information

ABSTRACT: The first elementary step of $Pd^{(0)}$-catalyzed cross-coupling involves the activation of an aryl halide by a $Pd^{(0)}$ catalyst, which is widely assumed to proceed in a formal 2-electron process, involving concerted cleavage of the aryl halide bond and formation of an aryl-Pd bond as to generate a $Pd^{(II)}$ complex. Contrary to common reactivity assumptions under this mechanistic manifold, we observed that severe steric hindrance in the aryl halide and catalyst did not inhibit the thermal activation of the aryl halide but instead greatly accelerated it, giving full conversion of an *ortho*,*ortho*-di-*tert*-butyl-substituted aryl bromide in 1 min at room temperature on gram scale with a bulky $Pd^{(0)}$ catalyst. Our mechanistic data revealed that a 1-electron-based halogen abstraction by $Pd^{(0)}$ is operative in such sterically demanding settings.

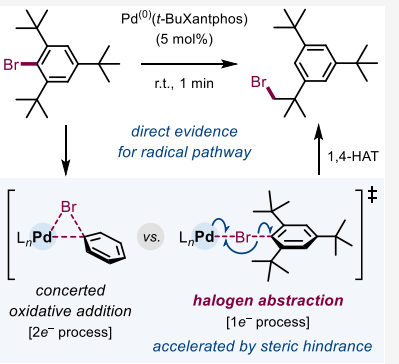

Downloaded via RWTH AACHEN HOCHSCHUL BIBL on September 24, 2025 at 14:55:01 (UTC).
See https://pubs.acs.org/sharingguidelines for options on how to legitimately share published articles.

INTRODUCTION

The palladium-catalyzed cross-coupling reaction stands as one of the most indispensable and widely employed chemical transformations worldwide, a status underscored by its recognition with the 2010 Nobel Prize in Chemistry.[1] It has profoundly shaped synthetic strategies and continues to drive innovation across both industry and academia. At its core, the reaction operates through a multistep mechanism, wherein the initial elementary step - the activation of the aryl halide - plays a decisive role in governing the overall reaction rate, substrate scope, and selectivity.[2]

Today's view of its mechanism primarily dates back to in-depth studies conducted in the 1970s and 1980s with the available catalyst/ligand of that time, *i.e.*, triphenylphosphine (PPh_3).[3] While the product of aryl halide activation was unambiguously confirmed as a $Pd^{(II)}$ complex, several 1- and 2-electron processes were initially considered as a mechanistic possibility of its formation, such as single electron transfer, nucleophilic aromatic substitution, or oxidative addition (Figure 1). Ultimately, kinetic and Hammett studies of the stoichiometric reaction of $Pd^{(0)}(PPh_3)_4$ with aryl halides were consistent with a concerted insertion of $Pd^{(0)}$ into the Ar-X bond, and oxidative addition (2-electron process) became the dominant paradigm.[4] The corresponding transition state for aryl halide activation by $Pd^{(0)}L_n$ was first computationally characterized over a decade later[5] and has seen continued studies since then,[6] especially with regard to the metal's ligation state.[2b,7] The oxidative addition mechanism is also assumed for substrates with additional steric bulk in close proximity to the $C(sp^2)$-X reaction center, and the steric hindrance is generally assumed to decrease the reactivity of oxidative addition.[2a,b,4a] Indeed, Pd-catalyzed cross-couplings of sterically demanding aryl halides often fail or have diminished efficiency.

Here, we present our findings that, contrary to currently prevailing assumptions, severe steric hindrance in the aryl halide and catalyst does not necessarily inhibit the thermal activation of the aryl halide but instead can greatly accelerate it. This counterintuitive reactivity was identified to be due to an unprecedented 1-electron process being favored in the thermal activation of an aryl halide with a $Pd^{(0)}$ catalyst over the generally assumed oxidative addition. These results indicate that steric hindrance either in the substrate or when used as a design principle in catalyst development can alter the course of the first elementary step of the ubiquitously employed Pd-catalyzed cross-coupling.

RESULTS & DISCUSSION

Assessment of Steric Effects in Pd Catalysis. In line with the general belief that the first elementary step of Pd-catalyzed cross-coupling would be inhibited by steric hindrance, our study of the coupling of an *ortho*- versus

Received: March 16, 2025
Revised: April 25, 2025
Accepted: May 14, 2025
Published: May 29, 2025

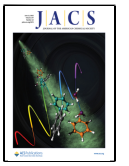

© 2025 The Authors. Published by American Chemical Society

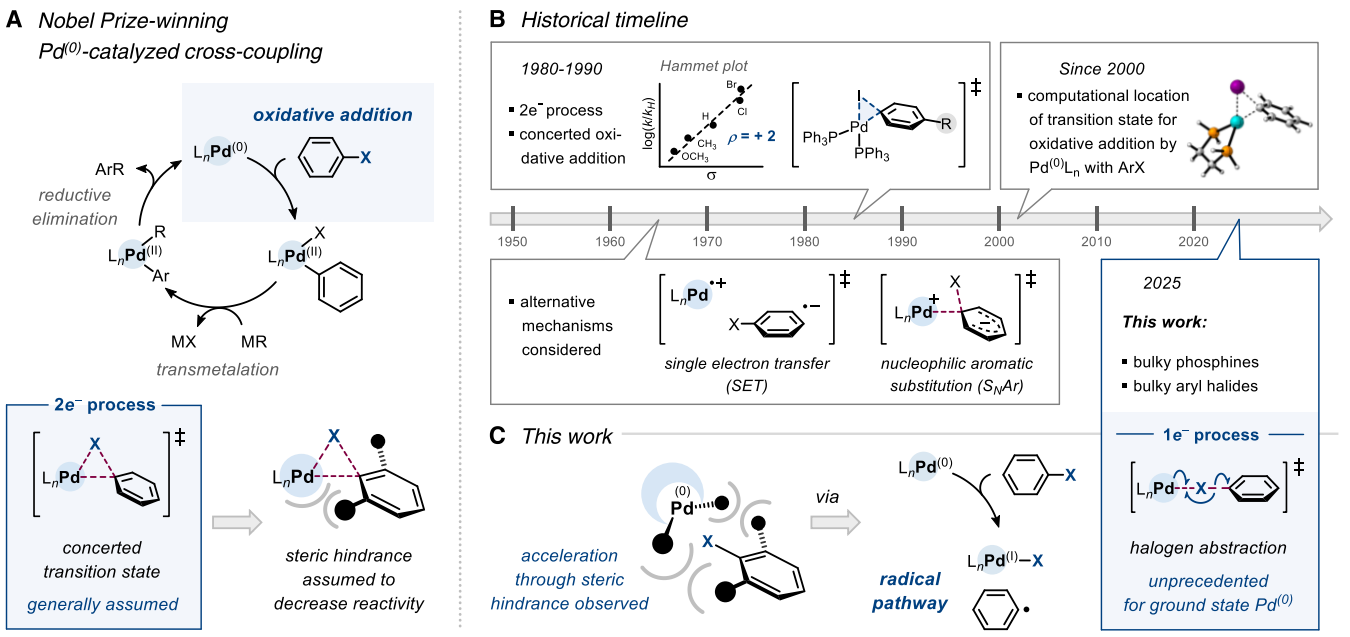

Figure 1. Activation of aryl halides by palladium. (A) First elementary step of Pd-catalyzed cross-coupling: general assumptions. (B) Mechanistic milestones. (C) Discovery of 1-electron reactivity enabled by steric hindrance.

para-tert-butyl-substituted aryl bromide, *i.e.*, **1a** and **1b** (Figure 2), with an organozinc reagent shows good conversion (98 and 46% after 4.5 h) to the corresponding coupling product **2b** at room temperature for the nonhindered aryl bromide (**1b**), while the *ortho*-substituted **1a** does not undergo any coupling whatsoever when using Pd catalysts with the ligands Xantphos or PCy_3 (Figure 2A).

Our computational studies of the corresponding oxidative addition transition states (2-electron process) by $Pd^{(0)}$(Xantphos) and $Pd^{(0)}(PCy_3)_2$ predict $\Delta\Delta G^{\ddagger}$ = 2.2 and 10.1 kcal/mol (at the CPCM (benzene) B3LYP-D3/def2-TZVP//CPCM (benzene) B3LYP-D3/6−31G(d)/LANL2DZ level of theory) in favor of addition at the less hindered site (Figure 2B), which is in line with current reactivity assumptions.

In stark contrast, when we further increased the steric bulk around the reaction center by replacing the phenyl substituents in Xantphos with more crowded *tert*-butyl groups, *i.e.*, employing 0.5 mol % Pd_2dba_3 with 1 mol % *t*-BuXantphos as a catalyst, this led to similar conversion (and product evolution over time) for the hindered and nonhindered aryl bromide in the cross-couplings with 4-fluorophenylzinc chloride at room temperature.

In other words, an increase in steric hindrance in the catalyst leads to enhanced reactivity of the sterically more crowded substrate. This finding deviates from what is typically expected in a two-electron oxidative addition mechanism. While the other elementary steps are likely contributing to the observed reactivity and may even govern selectivity under these sterically congested conditions, the observation that the most sterically demanding ligand (*t*-BuXantphos) promotes reaction with the bulkiest substrate is unexpected since both oxidative addition and transmetalation would be expected to be hindered in this instance. These findings prompted us to consider whether an alternative mechanistic pathway might be operative.

To proceed with studies of potential ArBr activation, knowledge of the likely active Pd species is critical. We hence examined the ligation state of $Pd^{(0)}$ with *t*-BuXantphos and synthesized the corresponding $Pd^{(0)}$ complex from a cyclooctadiene (COD) bound $Pd^{(II)}$ precursor (Pd(COD)-$(CH_2SiMe_3)_2$),[8] which upon coordination of a phosphine ligand expels COD and reductively eliminates bis-(trimethylsilyl)ethane. This led to the characteristic ^{31}P NMR signal of 42.7 ppm as an exclusive signal in benzene-d_6, and crystallization and X-ray crystallography revealed a $Pd^{(0)}$ complex with only a single *t*-BuXantphos ligand bound to it (see Scheme 1A). For comparison, the less bulky Xantphos forms a Pd(Xantphos)$_2$ complex.[9] However, the 'reactive species' (*i.e.*, the active species undergoing oxidative addition) is for Xantphos also a monophosphine, *i.e.*, $Pd^{(0)}$(Xantphos)$_1$ species, which, given the bidentate nature of the ligand, renders the active species overall bisligated (as it would also be for, *e.g.*, PPh_3).

Evaluation of Radical Pathway. Potential alternatives to the 2-electron oxidative addition mechanism for aryl bromide activation could be (i) the 1-electron process of halogen abstraction or (ii) single electron transfer. Since no reaction was seen in the absence of a Pd catalyst, the organometallic cross-coupling partner does not induce a SET process. Additionally, high energetic penalties of larger than 50 kcal/mol were calculated for a potential SET process from catalyst to substrate (see the SI, Table S3 for details), making SET as the underlying pathway and origin of reactivity divergence unlikely.

In a halogen abstraction pathway, the $Pd^{(0)}$ complex interacts with halogen, being aligned to donate electron density into the antibonding σ^* orbital of the C(sp^2)-Br bond.[2d] As a first approximation of the uppermost barrier of halogen abstraction, the minimum-energy crossing point (MECP) of singlet and triplet states of L_nPd−ArBr complex is determined,[10] which corresponds to the lowest-energy geometry of the system at which both electronic states have the same energy.[11] While this state is a good approximation of the underlying bond cleaving and forming events as well as associated charge transfer, previous studies in the context of Ni-catalysis found that the actual transition state (TS) for

https://doi.org/10.1021/jacs.5c04407
J. Am. Chem. Soc. 2025, 147, 19941−19948

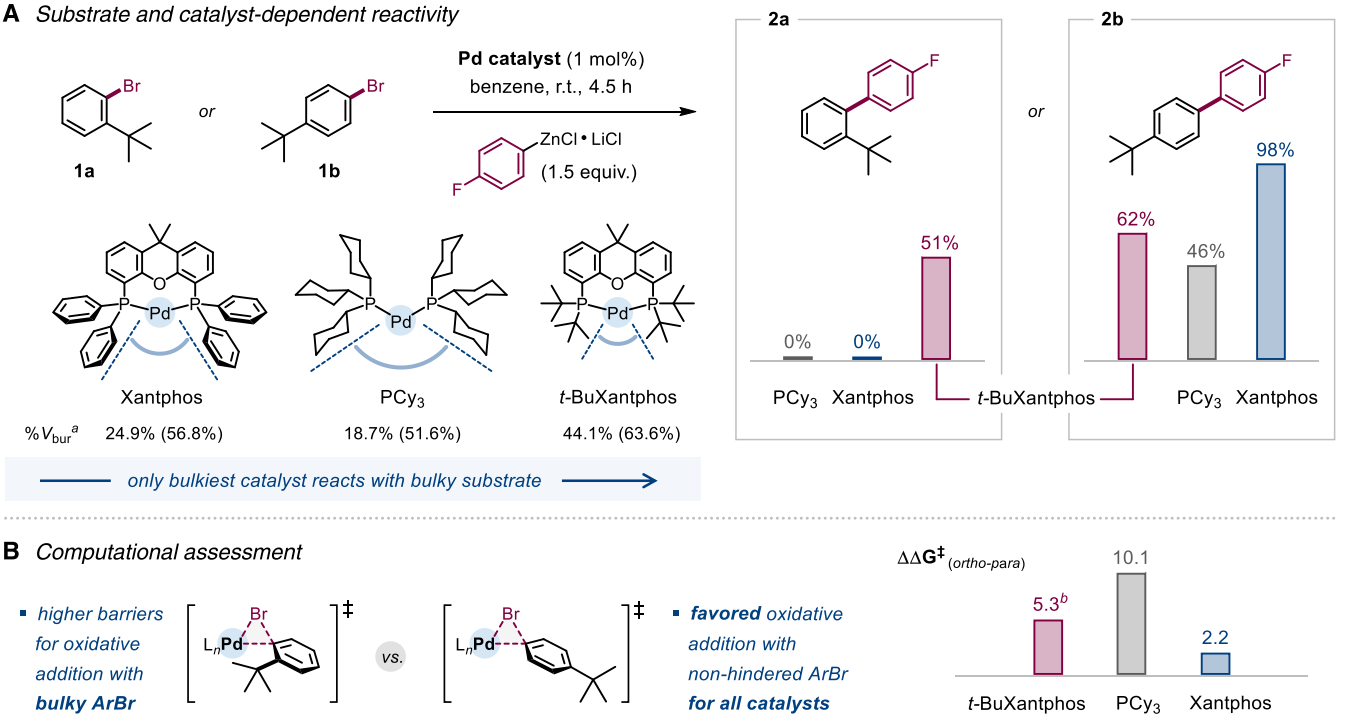

Figure 2. Counterintuitive reactivity in cross-coupling. (A) Experimental outcome. Reaction conditions: **1a** or **1b** (0.1 mmol), (4-F-Ph)ZnCl·LiCl (0.15 mmol), [Pd] catalyst (1 mol %), benzene (1 mL), r.t., 4.5 h. Yields were determined by ^{19}F NMR vs α,α,α-trifluorotoluene as an internal standard. [a]Percentage of buried volume in the front-facing half of the ligand sphere, total $\%V_{bur}$ in parentheses (for details, see SI). (B) Differences in computed Gibbs free energy barriers for concerted oxidative addition of **1a** vs **1b** ($\Delta\Delta G^{\ddagger}$) at the CPCM (benzene) B3LYP-D3/def2-TZVP//CPCM (benzene) B3LYP-D3/6−31G(d)/ LANL2DZ level of theory. [b]Highest barrier is the associative displacement of aryl bromide at Pd prior to oxidative addition (for details, see the SI).

halogen abstraction is lower in energy than the MECP.[10] The halogen abstraction TS exhibits a broken-symmetry, open-shell singlet configuration, which is computationally challenging to locate owing to its multiconfigurational nature. Indeed, it has so far never been located for Pd with an aryl halide but has been located for alkyl halides.[2d] That said, despite the likely overestimation of the halogen abstraction barrier with the MECP approximation, we consistently calculated a $\Delta\Delta G^{\ddagger}$ = 7.1 − 9.7 kcal/mol lower barrier for halogen abstraction over oxidative addition (2-electron process) for the hindered bromide **1a** with Pd$^{(0)}$(*t*-BuXantphos) for a range of different density functional theory (DFT) methods. A detailed account of method evaluation and benchmarking is found in the SI (Table S6).

On the other hand, for PCy_3 and Xantphos, the 2-electron oxidative addition is favored over halogen abstraction for **1a**, as it is for all studied catalysts with the less hindered substrate **1b**.

These data suggest that a different mechanism might in fact become feasible in the case of enhanced steric interaction instead of the commonly assumed 2-electron oxidative addition and that this may be a contributor to the similar product evolutions observed for the hindered and nonhindered substrates **1a** and **1b** with the *t*-BuXantphos-bound Pd$^{(0)}$ complex.

Direct Experimental Support for a Radical Pathway. Thus far, there has not been a case identified in which a ground-state Pd$^{(0)}$ complex (in the absence of any activation by light) would unambiguously favor a 1-electron process in the activation of the aryl halide over the generally assumed oxidative addition. Recently, Murphy and co-workers reported indirect support of likely aryl radical formation in reactions of aryl iodides in benzene at 130 °C in the presence of catalytic amounts of Pd complexes and 2 equiv of KO(*t*-Bu) base; it remains unclear however if the radical is generated from a labile Pd$^{(II)}$ oxidative addition complex under these conditions or originated in the activation of the aryl halide.[12] This contrasts the field of Ni-catalysis, where 1-electron processes, *e.g.*, *via* reductions (SET) or halogen abstraction of aryl halides to ArH have historic precedence and where Ni$^{(I)}$ complexes possess pronounced stabilities over Ni$^{(II)}$.[13]

However, since stoichiometric reactions between Pd$^{(0)}$(*t*-BuXantphos) and either **1a** or **1b** resulted only in the recovery of the starting materials, and the formation of coupling product **2** (as shown in Figure 2A) arises from a multistep cross-coupling process — involving aryl halide activation, transmetalation, and reductive elimination, the observed outcome likely reflects the cumulative influence of steric effects across all individual steps. To more clearly assess the aryl halide activation step in isolation, independent of a cross-coupling partner, we therefore sought a less ambiguous test system.

The 1-electron pathway would involve the abstraction of a halogen atom by Pd$^{(0)}$ to form an aryl radical and a Pd$^{(I)}$-X, which would be very prone to recombine to the corresponding Pd$^{(II)}$-aryl complex, *i.e.*, the same complex that would arise from a 2-electron oxidative addition.

To unambiguously single out a potential radical-based activation,[12] there is hence a need to outcompete the recombination of Pd$^{(I)}$ and aryl radical with alternative diagnostic reactivity. To this end, we considered 2-bromo-1,3,5-tri-*tert*-butylbenzene **4**. Substrate **4** is not only severely bulky around the C(sp^2)-Br reaction center, but it is also well established that any aryl radical formed undergoes extremely

https://doi.org/10.1021/jacs.5c04407
J. Am. Chem. Soc. 2025, 147, 19941−19948

Scheme 1. Reactivity of Pd(*t*-BuXantphos) (3). (A) Synthesis and X-ray Structure of 3. (B) Reactivity of 3 with 2-Bromo-1,3,5-tri-tert-butylbenzene (4). (C) Proposed Mechanism. (D) Computational Analysis of Competing Pathways[a]

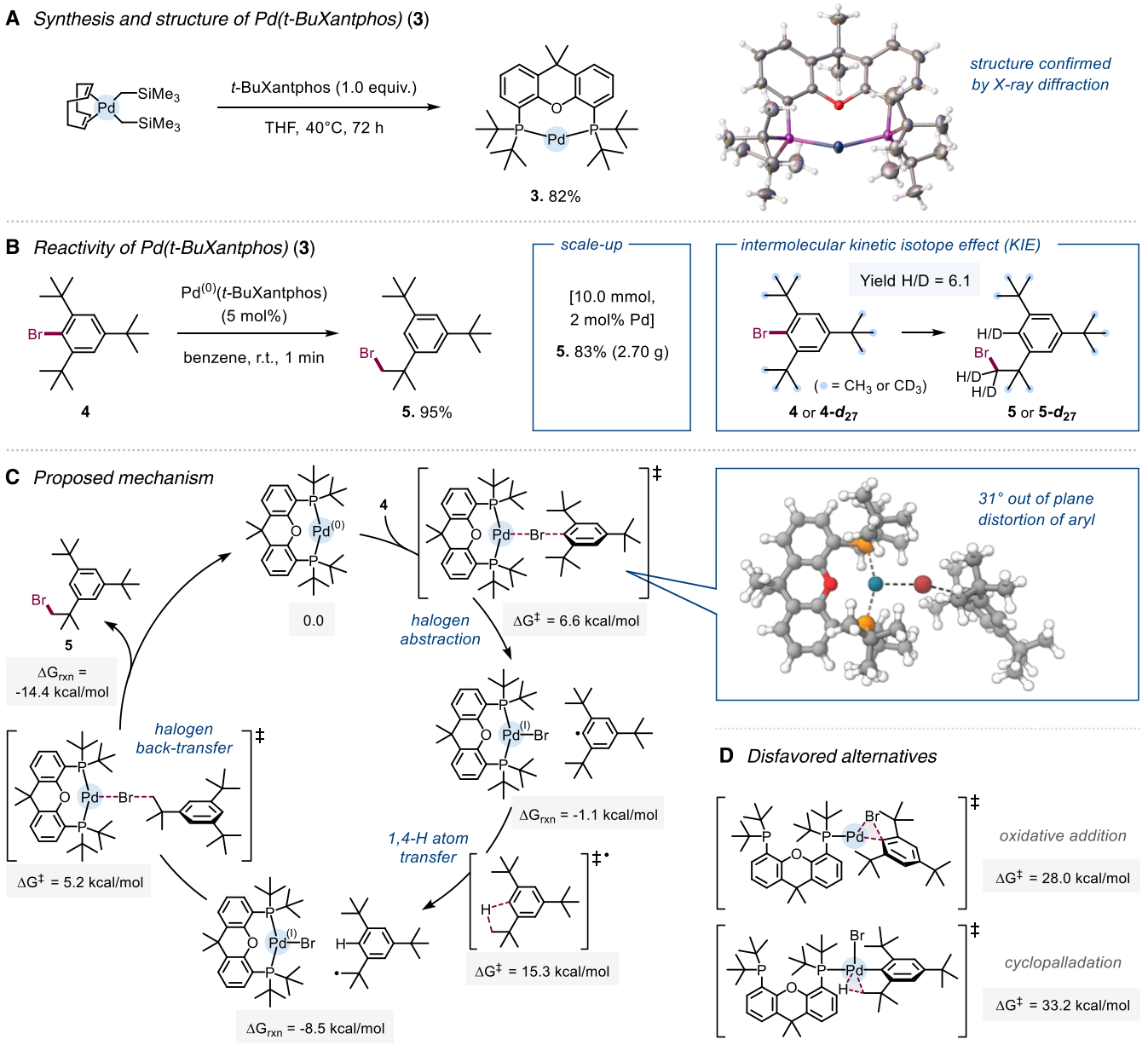

[a]Gibbs free energies (in kcal/mol; relative to **3**) at the CPCM (benzene) B3LYP-D3/def2-TZVP//CPCM (benzene) B3LYP-D3/6−31G(d)/LANL2DZ level of theory (for details, see the SI).

rapid 1,4-H atom transfer.[14] It is, hence, a diagnostic test to probe for the intermediacy of an aryl radical.

Interestingly, when we subjected 5 mol % of Pd(*t*-BuXantphos) catalyst to substrate **4** in benzene at room temperature (Scheme 1B), full conversion to the single product **5** (95% yield) was seen within 1 min reaction time. Formally, an intramolecular halogen atom transfer from aryl to alkyl had taken place in quantitative yield, which is unparalleled reactivity. The extreme speed is remarkable considering the severe steric bulk in the reactant and catalyst and is entirely at odds with general reactivity expectations in a conventional Pd-catalyzed cross-coupling and oxidative addition sense. The reactivity was just as high on a larger scale, *i.e.*, using 3.25 g of **4** (10 mmol), and the product could be isolated in 83% yield, using just 2 mol % of the catalyst and a reaction time of 1 min.

We therefore next turned to computational studies and mapped the reaction pathway for a potential halogen abstraction pathway (Scheme 1C) in comparison to a $Pd^{(0)}/Pd^{(II)}$ conventional 2-electron process (Scheme 1D). As expected for a traditional oxidative addition pathway, the 2-electron process required a high initial activation barrier for an oxidative addition of 27.2 − 31.1 kcal/mol, depending on the level of theory.[15] A subsequent C−H palladation at the $Pd^{(II)}$ oxidative addition intermediate is predicted to be of similar or even greater activation-free energy barrier (24.0−36.7 kcal/mol). In line with these computed barriers, analogous C−H activation processes require high temperatures to proceed.[16] Subsequent arene elimination (Ar−H), followed by C(sp^3)-Br

https://doi.org/10.1021/jacs.5c04407
J. Am. Chem. Soc. 2025, 147, 19941−19948

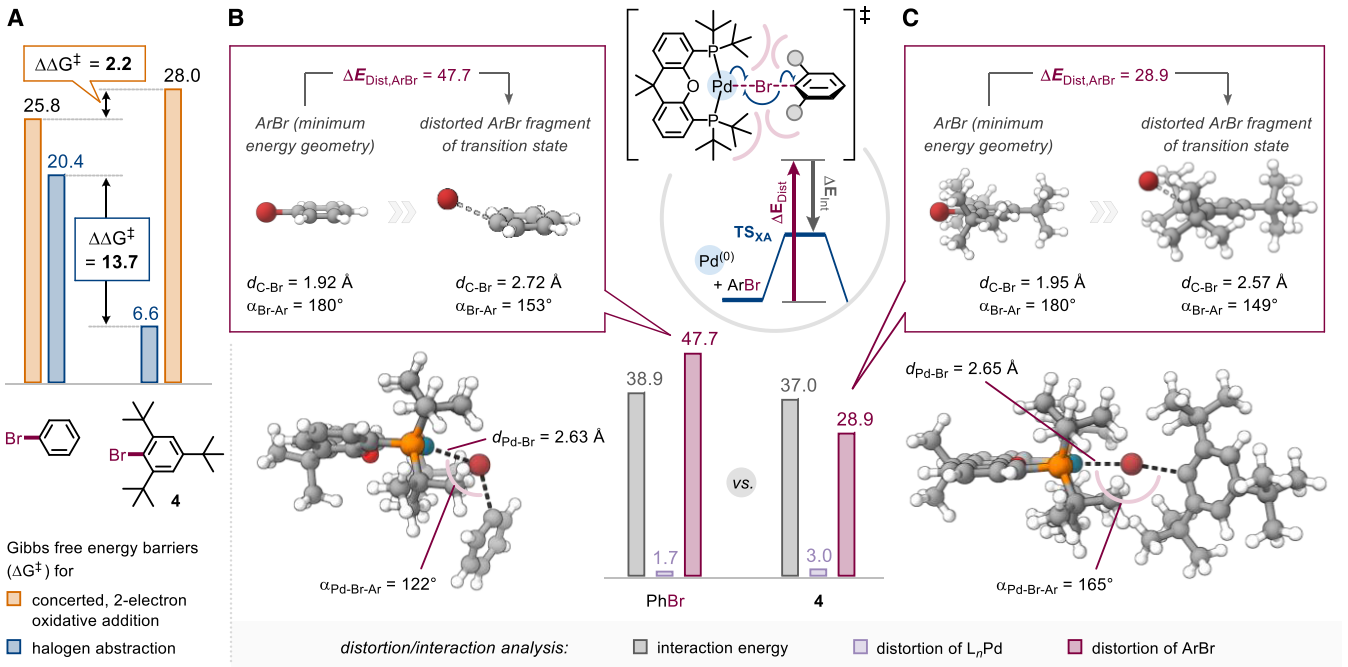

Figure 3. Distortion-interaction analysis of halogen abstraction transition states. (A) Calculated barriers for 1- vs. 2-electron processes for crowded and unsubstituted bromobenzene. (B) Halogen abstraction of bromobenzene. (C) Halogen abstraction of 2-bromo-1,3,5-tri-*tert*-butylbenzene (**4**). Electronic energies (in kcal/mol; relative to **3**), at the CPCM (benzene) B3LYP-D3/def2-TZVP//CPCM (benzene) B3LYP-D3/6-31G(d)/LANL2DZ level of theory.

elimination, could in principle yield the observed product **5**, but the associated activation barriers are high and inconsistent with the extremely rapid (1 min) reactivity observed at room temperature with Pd(*t*-BuXantphos) and **4**.

We hence considered the alternative halogen abstraction mechanism next and set out to locate the true transition state for halogen abstraction by Pd(*t*-BuXantphos), *i.e.*, the broken-symmetry, open-shell singlet transition state. We ultimately succeeded in calculating this transition state with DFT (at the CPCM (benzene) B3LYP-D3/6−31G(d)/LANL2DZ level of theory), which constitutes the first location of such a transition state for an aryl halide with Pd. The TS is illustrated in Scheme 1C. The Ar−Br bond is visibly stretched and distorted (2.57 Å length in TS vs 1.95 Å in ArBr) and bent out of plane by 30.8°, while the Pd fragment is barely distorted relative to its starting Pd catalyst.

Orbital analysis shows the direct interaction of an occupied 4d orbital of Pd with the empty σ^* orbital of the C−Br bond, generating two singly occupied orbitals, in accordance with a homolytic bond cleavage. SOMO1 is located on Pd (54.9%), with smaller contributions on the Br (16.2%) and P (18.9%), while SOMO2 is mainly located on the *ipso*-C(sp^2) of the arene (70.0%) and Br (8.9%) (see Figure S2 in the SI). This kind of orbital interaction differs from the one observed at the concerted oxidative addition transition state, where premixing of σ^* and π^* orbitals of aryl halide C-X bond is necessary to generate a hybrid orbital that then interacts with the Pd 4d orbital.[17] The halogen abstraction is calculated to have a relatively low barrier of 5.7 − 10.9 kcal/mol, depending on the level of theory.[15] It is consistently lower than oxidative addition, by $\Delta\Delta G^{\ddagger}$ = 16.2 − 24.6 kcal/mol, for a variety of DFT methods and $\Delta\Delta G^{\ddagger}$ = 19.3 kcal/mol at NEVPT2/CASSCF(18,14) level of theory (see the SI for details).

The subsequent H-atom abstraction can in principle occur *via* tunneling, which is of significance however merely at very low temperatures (below − 26 °C).[14] The calculated barrier for C−H atom abstraction is 13.3 − 19.1 kcal/mol, depending on the level of theory,[15] and hence predicted to be higher than the initial halogen abstraction. The final reabstraction of Br from $Pd^{(I)}$-Br to yield **5** is calculated to be similarly feasible and very facile (barrier of 2.3 − 5.6 kcal/mol).

The computed profile suggests that intramolecular H atom abstraction is the highest barrier step. We hence considered a deuterated analogue next and prepared **4**-d_{27} in which all methyl groups are CD_3 (Scheme 1B). The corresponding Br-atom relocated product **5**-d_{27} showed a roughly 6 times lower conversion under otherwise identical conditions (and reaction time) to its nondeuterated counterpart, which is fully in line with the C−H/D abstraction step being rate-determining. Our calculation of the kinetic isotope effect predicts a KIE of 6.2, which is in line with the experimental findings (Scheme 1B).

The collected data strongly supports a radical pathway and constitutes the first direct evidence of a 1-electron-based aryl halide activation by ground-state $Pd^{(0)}$. It also constitutes the first computational characterization of a halogen abstraction TS for the activation of an aryl halide with $Pd^{(0)}$.

Otherwise, 1-electron processes are proposed under light irradiation,[18,19] and we next investigated the reactivity of typical light-activated $Pd^{(0)}$ processes for probe **4**. Application of the published conditions by Gevorgyan[20] and Lautens[21] to substrate **4** gave after 20 h reaction time 17% (with the reported base) or 18% (without base) of alkyl bromide **5** along with dehalogenated products with $Pd(PPh_3)_4$, but no formation of **5** at all with Pd/DPEphos. As such, the ground-state $Pd^{(0)}$ 1-electron reactivity observed with *t*-BuXantphos is distinct, significantly higher in reactivity, and yielding a single product selectively.[22]

Our computational studies predict that for the highly congested aryl bromide **4**, the halogen abstraction pathway remains energetically favored over the conventional two-

https://doi.org/10.1021/jacs.5c04407
J. Am. Chem. Soc. 2025, 147, 19941−19948

electron oxidative addition, even with alternative ground-state $Pd^{(0)}$ catalysts such as $Pd[P(t\text{-}Bu)_3]_2$ or $Pd(PCy_3)_2$ by 13.5 − 21.6 kcal/mol.[23] This prediction is supported experimentally: stoichiometric reactions of compound **4** with $Pd[P(t\text{-}Bu)_3]_2$ and $Pd(PCy_3)_2$ yielded product **5** in 53% yield at 60 °C (for $P(t\text{-}Bu)_3$) and 26% yield at room temperature (for PCy_3), respectively. Furthermore, our calculations indicate that this preference for halogen abstraction is not dependent on the nature of the carbon−halogen bond, with analogous trends seen for C−I and C−Cl bonds (see Supporting Information for details).[24]

Distortion-Controlled Reactivity. Collectively, these data indicate that for reactions under severe steric hindrance, the halogen abstraction becomes a viable and favored reaction path. Interestingly, the effect of steric crowding is relatively modest on the barrier of oxidative addition (raising the barrier only by 2.2 kcal/mol for bromobenzene versus 2-bromo-1,3,5-tri-*tert*-butylbenzene **4** in reaction with Pd(*t*-BuXantphos); see Figure 3A and the SI, section 6.7). Instead, the steric crowding significantly lowers the barrier for halogen abstraction by Pd(*t*-BuXantphos), making it an extremely rapid room temperature process for one of the most sterically demanding cases of *ortho*,*ortho*-di-*tert*-butyl aryl bromide. Indeed, our calculation of bromobenzene by comparison indicates that halogen abstraction is 11.3 − 13.7 kcal/mol higher in barrier than for **4**.

What is the origin of this barrier difference? To gain insight, we conducted a distortion-interaction analysis of the halogen abstraction transition states by Pd(*t*-BuXantphos) for the bulky substrate **4** versus bromobenzene (Figure 3B−C). To this end, the transition state energies were dissected into their component energies, *i.e.*, the energies required to distort (ΔE_{Dist}) the geometries toward the transition state and the energy that is associated with the interaction of these distorted fragments (ΔE_{Int}), also known as the activation-strain model.[25] The results are shown in Figure 3 (for details, see section 6.8 in the SI). Interestingly, regardless of the substrate (bulky *ortho*,*ortho*-di-*tert*-butyl aryl bromide **4** or bromobenzene), the energy required to distort the Pd complex to the TS geometry is relatively low in both cases (1.7 versus 3.0 kcal/mol), and the corresponding interaction energies of the distorted substrates with the Pd catalyst are similar (38.9 vs 37.0 kcal/mol).

However, the substrate distortion energies are severely different: the hindered aryl bromide exhibits significantly lower distortion energy (28.9 kcal/mol, Figure 3C) than the nonhindered one (47.7 kcal/mol, Figure 3B).[26] This enhanced substrate distortion correlates with the latter transition state for bromobenzene. In line with this, the free energy change for bond dissociation (*i.e.*, homolytic scission) is also relatively low (64.1 kcal/mol), *i.e.*, 15.8 kcal/mol lower than for bromobenzene (79.9 kcal/mol) at the CBS-QB3 level of theory.[27]

Lower BDE of sterically hindered aryl halides and associated rate differences in halogen abstraction by Bu_3Sn-radical have previously been ascribed to a 'buttressing effect' in free radical chemistry.[28] Following Bickelhaupt's protocol,[29] our in-depth analysis of the origin of lower bond strength revealed that it is caused primarily by aryl bromide destabilization (see the Supporting Information, section 6.9). The *ortho*-*tert*-butyl substituents destabilize the aryl bromide more strongly than the corresponding radical relative to its nonsubstituted counterparts, which is also reflected in an elongated C−Br bond length in **4**, relative to bromobenzene (C−Br bond length is 1.95 Å, compared to 1.92 Å in PhBr, see Figure 3).

The bond dissociation free energy difference of bromobenzene and the bulky substrate **4** is 15.8 kcal/mol, which correlates well with the barrier difference for halogen abstraction ($\Delta\Delta G^{\ddagger}$ = 11.3 − 13.7 kcal/mol, depending on the level of theory).[15] The accelerating effect of steric crowding in these transformations and the halogen atom abstraction becoming vastly favored (over oxidative addition), hence, are primarily due to aryl halide destabilization in a distortion-controlled reactivity scenario.

CONCLUSIONS

In summary, this study challenges the prevailing paradigm that $Pd^{(0)}$ catalysts activate aryl halides exclusively *via* a two-electron process under thermal reaction conditions. Instead, we provide the first direct evidence of a 1-electron, radical-based thermal activation pathway. This reactivity is enabled by extreme steric hindrance, which significantly accelerates the halogen abstraction process. Given that the resulting aryl radical and $Pd^{(I)}$ intermediate are predisposed to rapidly recombine into a $Pd^{(II)}$ complex - unless alternative exit pathways are accessible as designed for substrate **4** - this mechanistic paradigm may have far-reaching implications across the Pd-catalysis landscape and alternative second-row metals for which oxidative addition is likewise generally assumed. Moving forward, our research aims to systematically map the scope of this radical activation mechanism in metal catalysis and develop predictive frameworks to guide its recognition (as a function of substrate or ligand bulkiness) and tailored applications in catalysis.

ASSOCIATED CONTENT

Supporting Information

The Supporting Information is available free of charge at https://pubs.acs.org/doi/10.1021/jacs.5c04407.

Experimental procedures and characterization data of compounds (PDF)

Accession Codes

Deposition Number 2402811 contains the supplementary crystallographic data for this paper. These data can be obtained free of charge *via* the joint Cambridge Crystallographic Data Centre (CCDC) and Fachinformationszentrum Karlsruhe Access Structures service.

AUTHOR INFORMATION

Corresponding Author

Franziska Schoenebeck − *Institute of Organic Chemistry, RWTH Aachen University, 52074 Aachen, Germany;* orcid.org/0000-0003-0047-0929; Email: franziska.schoenebeck@rwth-aachen.de

Authors

Daniel Hupperich − *Institute of Organic Chemistry, RWTH Aachen University, 52074 Aachen, Germany;* orcid.org/0009-0002-3724-3228

Jaime Ponce-de-León − *Institute of Organic Chemistry, RWTH Aachen University, 52074 Aachen, Germany;* orcid.org/0000-0001-7464-2469

Ignacio Funes-Ardoiz − *Institute of Organic Chemistry, RWTH Aachen University, 52074 Aachen, Germany;* orcid.org/0000-0002-5843-9660

Theresa Sperger − *Institute of Organic Chemistry, RWTH Aachen University, 52074 Aachen, Germany;* orcid.org/0000-0002-3870-9870

Complete contact information is available at: https://pubs.acs.org/10.1021/jacs.5c04407

Notes

The authors declare no competing financial interest.

■ ACKNOWLEDGMENTS

We thank the European Research Council, the Fonds der Chemischen Industrie (scholarship to D.H.), and the Alexander von Humboldt Foundation (fellowship to I.F.A.) for funding. Calculations were performed with computing resources granted by JARA-HPC from RWTH Aachen University under project "jara0091".

■ REFERENCES

(1) (a) *New Trends in Cross-Coupling: Theory and Applications*; Colacot, T. J., Ed.; The Royal Society of Chemistry: Cambridge, UK, 2015. (b) *Transition Metal-Catalyzed Couplings in Process Chemistry: Case Studies From the Pharmaceutical Industry*; Magano, J.; Dunetz, J. R., Eds.; Wiley: Hoboken, NJ, 2013.

(2) (a) Hartwig, J. F. *Organotransition Metal Chemistry − from Bonding to Catalysis*; University Science Books: Sausalito, 2010. (b) Rio, J.; Liang, H.; Perrin, M.-E. L.; Perego, L. A.; Grimaud, L.; Payard, P.-A. We Already Know Everything about Oxidative Addition to Pd(0): Do We? *ACS Catal.* **2023**, *13*, 11399−11421. (c) Labinger, J. A. Tutorial on Oxidative Addition. *Organometallics* **2015**, *34*, 4784−4795. (d) Besora, M.; Maseras, F. The diverse mechanisms for the oxidative addition of C−Br bonds to $Pd(PR_3)$ and $Pd(PR_3)_2$ complexes. *Dalton Trans.* **2019**, *48*, 16242−16248.

(3) (a) Fitton, P.; Rick, E. A. The addition of aryl halides to tetrakis(triphenylphosphine)palladium(0). *J. Organomet. Chem.* **1971**, *28*, 287−291. (b) Fauvarque, J.-F.; Pflüger, F.; Troupel, M. Kinetics of oxidative addition of zerovalent palladium to aromatic iodides. *J. Organomet. Chem.* **1981**, *208*, 419−427.

(4) (a) Amatore, C.; Pflüger, F. Mechanism of oxidative addition of palladium(0) with aromatic iodides in toluene, monitored at ultramicroelectrodes. *Organometallics* **1990**, *9*, 2276−2282. (b) Casado, A. L.; Espinet, P. On the Configuration Resulting from Oxidative Addition of RX to $Pd(PPh_3)_4$ and the Mechanism of the cis-to-trans Isomerization of $[PdRX(PPh_3)_2]$ Complexes (R = Aryl, X = Halide). *Organometallics* **1998**, *17*, 954−959.

(5) Sundermann, A.; Uzan, O.; Martin, J. M. L. Computational Study of a New Heck Reaction Mechanism Catalyzed by Palladium-(II/IV) Species. *Chem. - Eur. J.* **2001**, *7*, 1703−1711.

(6) (a) Senn, H. M.; Ziegler, T. Oxidative Addition of Aryl Halides to Palladium(0) Complexes: A Density-Functional Study Including Solvation. *Organometallics* **2004**, *23*, 2980−2988. (b) Goossen, L. J.; Koley, D.; Hermann, H. L.; Thiel, W. Mechanistic Pathways for Oxidative Addition of Aryl Halides to Palladium(0) Complexes: A DFT Study. *Organometallics* **2005**, *24*, 2398−2410. (c) McMullin, C. L.; Fey, N.; Harvey, J. N. Computed ligand effects on the oxidative addition of phenyl halides to phosphine supported palladium(0) catalysts. *Dalton Trans.* **2014**, *43*, 13545−13556.

(7) Ahlquist, M.; Fristrup, P.; Tanner, D.; Norrby, P.-O. Theoretical Evidence for Low-Ligated Palladium(0): [Pd−L] as the Active Species in Oxidative Addition Reactions. *Organometallics* **2006**, *25*, 2066−2073.

(8) Pan, Y. Syntheses and spectroscopic characteristics of dialkylpalladium(II) complexes; $PdR_2(cod)$ as precursors for derivatives with N- or P-donor ligands. *J. Organomet. Chem.* **1999**, *577*, 257−264.

(9) (a) Klingensmith, L. M.; Strieter, E. R.; Barder, T. E.; Buchwald, S. L. New Insights into Xantphos/Pd-Catalyzed C−N Bond Forming Reactions: A Structural and Kinetic Study. *Organometallics* **2006**, *25*, 82−91. (b) Grushin, V. V.; Marshall, W. J. Facile Ar−CF_3 Bond Formation at Pd. Strikingly Different Outcomes of Reductive Elimination from $[(Ph_3P)_2Pd(CF_3)Ph]$ and [(Xantphos)$Pd(CF_3)$-Ph]. *J. Am. Chem. Soc.* **2006**, *128*, 12644−12645.

(10) (a) Funes-Ardoiz, I.; Nelson, D. J.; Maseras, F. Halide Abstraction Competes with Oxidative Addition in the Reactions of Aryl Halides with $[Ni(PMe_nPh_{(3-n)})_4]$. *Chem. - Eur. J.* **2017**, *23*, 16728−16733. (b) Nelson, D. J.; Maseras, F. Steric effects determine the mechanisms of reactions between bis(N-heterocyclic carbene)-nickel(0) complexes and aryl halides. *Chem. Commun.* **2018**, *54*, 10646−10649.

(11) Harvey, J. N.; Aschi, M.; Schwarz, H.; Koch, W. The singlet and triplet states of phenyl cation. A hybrid approach for locating minimum energy crossing points between non-interacting potential energy surfaces. *Theor. Chem. Acc.* **1998**, *99*, 95−99.

(12) Clark, K. F.; Tyerman, S.; Evans, L.; Robertson, C. M.; Nelson, D. J.; Kennedy, A. R.; Murphy, J. A. A Hierarchy of Ligands Controls Formation and Reaction of Aryl Radicals in Pd-Catalyzed Ground-State Base-Promoted Coupling Reactions. *J. Am. Chem. Soc.* **2023**, *145*, 20849−20858.

(13) (a) Tsou, T. T.; Kochi, J. K. Mechanism of oxidative addition. Reaction of nickel(0) complexes with aromatic halides. *J. Am. Chem. Soc.* **1979**, *101*, 6319−6332. (b) Pierson, C. N.; Hartwig, J. F. Mapping the mechanisms of oxidative addition in cross-coupling reactions catalysed by phosphine-ligated Ni(0). *Nat. Chem.* **2024**, *16*, 930−937.

(14) (a) Brunton, G.; Griller, D.; Barclay, L. R. C.; Ingold, K. U. Kinetic applications of electron paramagnetic resonance spectroscopy. 26. Quantum-mechanical tunneling in the isomerization of sterically hindered aryl radicals. *J. Am. Chem. Soc.* **1976**, *98*, 6803−6811. (b) Brunton, G.; Gray, J. A.; Griller, D.; Barclay, L. R. C.; Ingold, K. U. Kinetic applications of electron paramagnetic resonance spectroscopy. 32. Further studies of quantum-mechanical tunneling in the isomerization of sterically hindered aryl radicals. *J. Am. Chem. Soc.* **1978**, *100*, 4197−4200.

(15) Based on the geometries optimized at the CPCM (benzene) B3LYP-D3/6−31G(d)/LANL2DZ level of theory, different functionals were evaluated for energy calculation at CPCM (benzene) functional/def2-TZVP, where functional is B3LYP-D3, M06L, PBE0-D3 or TPSS-D3.

(16) (a) Lucas, E. L.; Lam, N. Y. S.; Zhuang, Z.; Chan, H. S. S.; Strassfeld, D. A.; Yu, J.-Q. Palladium-Catalyzed Enantioselective β-C(sp3)−H Activation Reactions of Aliphatic Acids: A Retrosynthetic Surrogate for Enolate Alkylation and Conjugate Addition. *Acc. Chem. Res.* **2022**, *55*, 537−550. (b) Wu, K.; Lam, N.; Strassfeld, D. A.; Fan, Z.; Qiao, J. X.; Liu, T.; Stamos, D.; Yu, J.-Q. Palladium (II)-Catalyzed C−H Activation with Bifunctional Ligands: From Curiosity to Industrialization. *Angew. Chem., Int. Ed.* **2024**, *63*, No. e202400509.

(17) Ariafard, A.; Lin, Z. Understanding the Relative Easiness of Oxidative Addition of Aryl and Alkyl Halides to Palladium(0). *Organometallics* **2006**, *25*, 4030−4033.

(18) (a) Juliá, F. Catalysis in the Excited State: Bringing Innate Transition Metal Photochemistry into Play. *ACS Catal.* **2025**, *15*, 4665−4680. (b) Liu, Q.; Dong, X.; Li, J.; Xiao, J.; Dong, Y.; Liu, H. Recent Advances on Palladium Radical Involved Reactions. *ACS Catal.* **2015**, *5*, 6111−6137.

(19) (a) Fusano, A.; Fukuyama, T.; Nishitani, S.; Inouye, T.; Ryu, I. Synthesis of Alkyl Alkynyl Ketones by Pd/Light-Induced Three-Component Coupling Reactions of Iodoalkanes, CO, and 1-Alkynes. *Org. Lett.* **2010**, *12*, 2410−2413. (b) Chuentragool, P.; Parasram, M.; Shi, Y.; Gevorgyan, V. General, Mild, and Selective Method for Desaturation of Aliphatic Amines. *J. Am. Chem. Soc.* **2018**, *140*, 2465−2468. (c) Torres, G. M.; Liu, Y.; Arndtsen, B. A. A dual light-driven palladium catalyst: Breaking the barriers in carbonylation reactions. *Science* **2020**, *368*, 318−323.

(20) Parasram, M.; Chuentragool, P.; Sarkar, D.; Gevorgyan, V. Photoinduced Formation of Hybrid Aryl Pd-Radical Species Capable of 1,5-HAT: Selective Catalytic Oxidation of Silyl Ethers into Silyl Enol Ethers. *J. Am. Chem. Soc.* **2016**, *138*, 6340−6343.

(21) Marchese, A. D.; Durant, A. G.; Reid, C. M.; Jans, C.; Arora, R.; Lautens, M. Pd(0)/Blue Light Promoted Carboiodination Reaction − Evidence for Reversible C−I Bond Formation via a Radical Pathway. *J. Am. Chem. Soc.* **2022**, *144*, 20554−20560.
(22) 9% of alkyl bromide 5 were obtained with $Pd(PPh_3)_4$ after 10 min, both with and without base.
(23) Calculated at the CPCM (THF) B3LYP-D3/def2-TZVP//CPCM (THF) B3LYP-D3/6−31G(d)/LANL2DZ level of theory. For details see the SI.
(24) We have explored the influence of different substituents in the para-position on the Gibbs free activation barrier of the 2-electron oxidative addition versus the one-electron halogen abstraction and found that both mechanisms are similarly impacted by the substituents (for details, please see the SI, section 6.10).
(25) Bickelhaupt, F. M.; Houk, K. N. Analyzing Reaction Rates with the Distortion/Interaction-Activation Strain Model. *Angew. Chem., Int. Ed.* **2017**, *56*, 10070−10086.
(26) This trend is analogous for alternative levels of theory. For details see the SI.
(27) For appropriateness of level of theory, see Zulueta, B.; Tulyani, S. V.; Westmoreland, P. R.; Frisch, M. J.; Petersson, E. J.; Petersson, G. A.; Keith, J. A. A Bond-Energy/Bond-Order and Populations Relationship. *J. Chem. Theory Comput.* **2022**, *18*, 4774−4794.
(28) Galli, C.; Pau, T. The dehalogenation reaction of organic halides by tributyltin radical: The energy of activation vs. the BDE of the C-X bond. *Tetrahedron* **1998**, *54*, 2893−2904.
(29) Blokker, E.; van Zeist, W.-J.; Sun, X.; Poater, J.; van der Schuur, J. M.; Hamlin, T. A.; Bickelhaupt, F. M. Methyl Substitution Destabilizes Alkyl Radicals. *Angew. Chem., Int. Ed.* **2022**, *61*, No. e202207477.

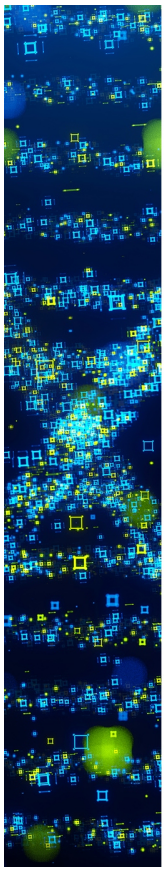
CAS BIOFINDER DISCOVERY PLATFORM™
STOP DIGGING THROUGH DATA —START MAKING DISCOVERIES
CAS BioFinder helps you find the right biological insights in seconds
Start your search
CAS
A division of the American Chemical Society

https://doi.org/10.1021/jacs.5c04407
J. Am. Chem. Soc. 2025, 147, 19941−19948